Jahn–Teller impurity dependence of the transition temperature T_{c1}, critical exponent and pseudo-Jahn–Teller potential well splitting in $ZnTiF_6 . 6H_2O$

D K De†

Department of Physics, PO Box 19059, The University of Texas at Arlington, Arlington, Texas 76019, USA

Abstract. The 182 K (−91.2 °C) trigonal-to-monoclinic phase transition in $ZnTiF_6 . 6H_2O$ single crystal has been studied by EPR, for various concentrations of doped Jahn–Teller (JT) impurity Cu^{2+} ions and also for non-JT impurity Ni^{2+} ions. The transition temperature T_{c1} which decreases with increase in impurity concentration, is more strongly affected by the JT impurity. The critical exponent β as well as the JT potential well splitting E_0 have been determined from the temperature variation in EPR signal intensity in the immediate neighbourhood of T_{c1} for the Cu^{2+} impurity. The critical exponent β and E_0 are dependent strongly on the JT impurity concentration. For two different concentrations of Cu^{2+} ions, i.e. 0.043 wt% and 0.98 wt%, the values of β are 0.5 ± 0.05 and 0.12 ± 0.03, respectively, while the values of E_0 are 140 ± 15 cm^{-1} and 97 ± 12 cm^{-1}, respectively. The value of E_0 for a deuterated crystal containing a low Cu^{2+} concentration is 78 ± 10 cm^{-1}. The decrease in E_0 with increasing Cu^{2+} concentration for a hydrated crystal and also with deuteration (for a low copper concentration) is in qualitative agreement with the corresponding gradual phase transition observed in these materials.

1. Introduction

The crystal zinc fluotitanate hexahydrate, $ZnTiF_6 . 6H_2O$ (ZTFH), belongs to the class of compounds having the general formula $ABF_6 . 6H_2O$ where A ≡ Zn, Mn, Ni, Co, Mg, etc and B ≡ Ti, Si, Ge, etc. The structure consists of nearly regular $A(H_2O)_6$ and BF_6 octahedra packed in a trigonally distorted structure similar to that of CsCl. Many compounds of the above series exhibit first-order structural phase transitions in the temperature range 130–300 K, from the high-temperature trigonal phase ($R\bar{3}m$) to the low-temperature monoclinic phase ($P2_1/c$) (Kodera *et al* 1972, Syoyama and Osaki 1972).

EPR measurements on ZTFH : Ni^{2+} by Rubins (1974) indicated the loss of high-temperature axial symmetry of $Zn(H_2O)$ octahedra below 182 K and the development of six inequivalent magnetic sites, each with a rhombic component; the spectra coincide with the pseudo-trigonal C axis. ^{19}F NMR studies (Afanasyev *et al* 1979) reveal a first-order phase transition at −91.2 °C (T_{c1}) when the rotation of the fluorine octahedra freezes and the single ^{19}F line splits into two, indicating the loss of a chemical equivalence

† Present address: Department of Radiology, Bowman-Gray School of Medicine, Wake Forest University, 300 South Hawthorne Road, Winston-Salem, NC 27103, USA.

C35

between the fluorine atoms following a tetragonal distortion of the TiF_6^{2-} octaheda. Chowdhury *et al* (1981) found a second weak transition of a continuous nature in ZTFH at 217 K. The latter transition is found to occur in $ZnTiF_6 . 6D_2O$ (ZTFD) at $-43\,°C$ (T_{c2}), where T_{c1} is not affected on deuteration. Recently, Chowdhury *et al* (1985) examined the temperature dependence of the Raman spectra of both ZTFH and ZTFD and found that some bands show an interesting behaviour near the transition temperature. The frequency of the symmetric stretching vibrational mode $\nu_s(H_2O-D_2O)$ in both ZTFH and ZTFD increases sharply by about $6\,cm^{-1}$ at the phase transition temperature as the crystal is cooled and then remains constant for the low-temperature phase. Das *et al* (1985) theoretically investigated the various coupling between the vibrational and rotational modes of TiF_6^{2-} and (M^{2+}, H_2O) octahedra. Chowdhury *et al* (1983) performed IR and Raman spectroscopy measurements and concluded that the librational modes of the water molecule change significantly around the transition temperature.

De *et al* (1984) performed EPR measurements on ZTFH : Cu^{2+} (Cu^{2+} substituting for some of the Zn sites). Cu^{2+} ions in this system have an orbitally degenerate ^2E ground state and the system exhibits a strong Jahn–Teller (JT) effect as confirmed by them. The JT stabilisation energy $E_{JT} = 1000\,cm^{-1}$ has been determined from a fit of the EPR linewidth, which varies exponentially with temperature, to an Orbach relaxation mechanism (De 1986). Further, from the gradual variation of the spin Hamiltonian parameters $g_\parallel, g_\perp, A_\parallel$ and $A_\perp$ down to 4.2 K, it has been concluded that one of the three JT potential wells is lower than the other two by an energy E_0 of $140\,cm^{-1}$. With a low Cu^{2+} concentration of 0.043 wt% the concentration temperature was lowered by 11 °C from that of pure ZTFH; T_{c1} was further lowered when the crystal was powdered.

Because of possible interaction between the soft mode driving the phase transition and the JT active modes, the JT effect in such systems is modified in comparison with those JT systems which do not exhibit any structural transition (De 1986), e.g. $ZnSiF_6 . 6H_2O$, MgO, CaO, $La_2Mg_3(NO_3)_{12} . 24H_2O$ doped with Cu^{2+}. Another interesting observation was that the spin–lattice relaxation rate $1/T_1$ was much slower in ZTFH : Cu^{2+} than in the latter systems.

In this paper, we report a systematic study of the dependence of the phase transition temperature T_{c1} on JT impurity, i.e. Cu^{2+}, concentration and compare it with that of non-JT impurity, i.e. Ni^{2+}, concentration in ZTFH. Further, we explore the dependence of the critical behaviour and the critical exponent β on JT impurity concentrations from EPR measurements in the immediate neighbourhood of the transition temperature. From such measurements, we have been able to determine also the JT potential splitting E_0. The decrease in E_0 with increase in Cu^{2+} concentration and deuteration is discussed and found to be consistent with the corresponding gradual phase transition observed in this material. Deviation from mean-field behaviour is observed for high concentrations.

2. Experimental details

Single crystals of ZTFH were grown by slow evaporation of an aqueous solution of $ZnTiF_6$ obtained by dissolving $ZnCO_3$ in 40% H_2TiF_6 : $CuCO_3$ and $NiCO_3$ were added to grow doped crystals of various concentrations. Recrystallisation was done to reduce the Mn^{2+} impurity concentration beyond the detection limit in these crystals. Unlike Cu^{2+} and Ni^{2+}, Mn^{2+} in these crystals produces a slight raising of T_{c1}. Only good single crystals devoid of any twinning and with uniform concentrations of Cu^{2+} were chosen for the experiments. These crystals were analysed by Galbraith Chemical Laboratories, USA,

estimation of the impurity concentration. For the phase transition study, EPR spectra were measured in the $(1\bar{1}0)$ plane of the crystal with the magnetic field direction along the g_{max} (this direction is close to the $g_\parallel$ direction or [100] direction of the Cu^{2+} ion and corresponds to the maximum g value in the $(1\bar{1}0)$ plane). Accuracy of determining the onset of phase transition is higher in this direction because of the appearance of as many as six lines with the largest field separations (De *et al* 1984).

Above T_{c1}, the EPR spectrum consists of an isotropic line only. It may be mentioned that it is not possible to determine the phase transition along the [111] direction because all the EPR lines remain coincident even after phase transition except for the appearance of four copper hyperfine lines at around 120 K. The EPR spectrometer used was a Q-band (33–35 GHz) reflectance spectrometer built in the laboratory. Temperatures were varied by a manual control. An approximately uniform cooling and heating rate of between 1 °C min^{-1} and 1 °C per 120 min could be attained. The sample could be maintained at any temperature above 77 K (liquid-N_2 temperature) to within ± 0.1 °C for 30 min. The temperature of the sample structure was measured by both E- and T-type thermocouples. The thermometers and the digital readouts were calibrated at the temperatures of liquid N_2, solid CO_2, a toluene-and-liquid-N_2 slush and a mixture of isopropane and solid CO_2.

3. Enhanced lowering of the phase-transition temperature T_{c1}

The transition temperature T_{c1} was recorded through the variation in the intensity I of the isotropic signal as the sample was cooled at a uniform rate of 3 °C h^{-1}. Increases up to about 1 °C above the phase transition. The sample is then cooled at a rate of 0.5 °C h^{-1}. T_{c1} during cooling can be noted by the appearance of the high-field lines or by a noticeable reduction in the isotropic EPR signal intensity I (as high as 60% in dilute material; see figures 1 and 5) with a temperature variation of ± 0.1 °C. In figure 1, it can be seen that at -102.6 °C there is a noticeable change in I from that at -102.5 °C. This is associated with the appearance of high-field signals which is prominent at -102.7 and -102.8 °C. So T_c for a Cu^{2+} concentration of 0.043 wt% could be recorded as -102.6 ± 0.2 °C (± 0.1 °C is the error in the temperature recording). It can be seen that both the high- and the low-temperature phases coexist over a finite temperature interval ΔT. ΔT is found to be concentration dependent. The isotropic signal vanishes a few degrees Celsius below T_{c1}. The anisotropic signals gain intensity as the sample is cooled. Hyperfine
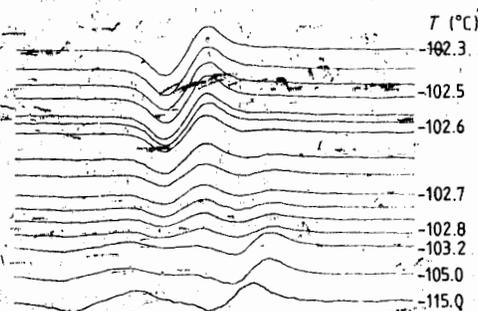

Figure 1. EPR spectra of ZTFH : Cu^{2+} recorded in the immediate neighbourhood of the phase transition temperature T_{c1} for a Cu^{2+} concentration of 0.043 wt%.
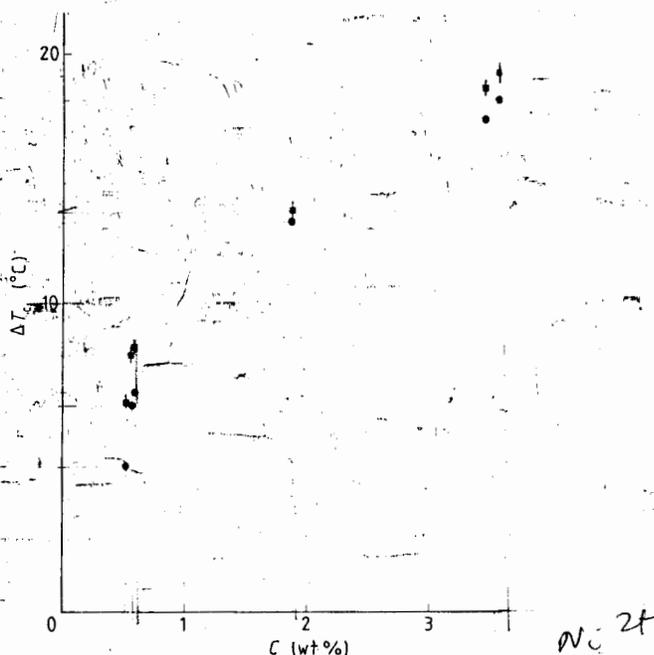
Figure 2. Decrease $\Delta T_c (= T_{c0} - T_{c1\,impurity})$ in the transition temperature T_{c1} from T_{c0} of pure ZTFH due to the additions of Cu^{2+} impurities ($T_{c0} = 182$ K): ●, on warming; ■, on cooling. The maximum error in T_{c1} for Cu^{2+} concentrations of less than 2 wt% is ± 1 °C while that for concentrations between 2 and 4 wt% is ± 3 °C. For the highest concentration, it is ± 6 °C.

structure appears at around 118 K. Both the g- and the A-values are temperature dependent down to 4.2 K.

During warming from the low-temperature phase, the transition is noticed by changes taking place in the reverse order. However, the transition temperature $T_{c1}\uparrow$ during warming from the low-temperature phase is slightly higher than the transition temperature $T_{c1}\downarrow$ during cooling from the trigonal phase. The decreases ΔT_c in $T_{c1}\downarrow$ and $T_{c1}\uparrow$ from the transition temperature T_{c0} of pure ZTFH for different concentrations are shown in figures 2 and 3. The decrease ΔT_c in T_{c1} from that of T_{c0} increases with both Cu^{2+} and Ni^{2+}. It is significantly higher for Cu^{2+} (JT impurity) than for Ni^{2+} (non-JT impurity) for the same concentration. The value of the transition temperature T_{c1} obtained is independent of the orientation of the crystal. The observed enhanced lowering of T_{c1} for a JT impurity in comparison with that for a non-JT impurity will be explained in a later paper.

4. Critical phenomena

As discussed earlier, the EPR signal intensity varies sharply in the neighbourhood of T_{c1} for low Cu^{2+} concentrations (the neighbourhood may be as small as 0.1 °C). However, as the Cu^{2+} concentration is increased, the transition is found to become gradual with respect to temperature (figure 4). The temperature interval ΔT over which both the phases coexist (trigonal R3m and monoclinic phases P2$_1$/c) widens with increase in the Cu^{2+} concentration. A high Cu^{2+} impurity concentration thus drives the phase transition
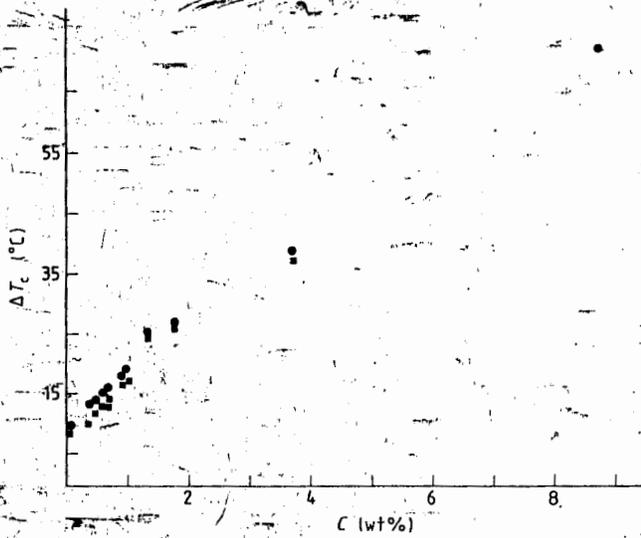
Figure 3. Decrease in the transition temperature T_{c1} from T_{c0} of pure ZTFH, due to the addition of Ni^{2+} impurities: ●, on warming; ■, on cooling.
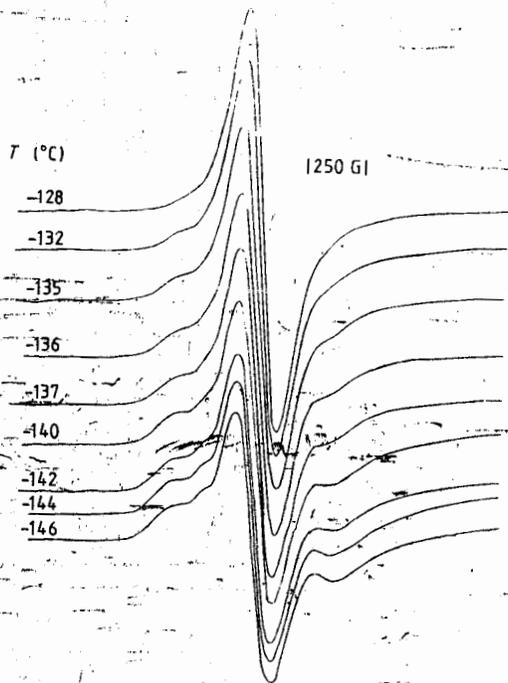

Figure 4. The EPR spectrum recorded for a Cu^{2+} concentration of 3.7 wt% in ZTFH. It is seen that the transition to the monoclinic phase (see text) takes place gradually with respect to the change in temperature in contrast with the sharp transition observed for low Cu^{2+} concentrations (see figure 1).

towards continuous or higher order (compare figures 1 and 4). To investigate the
of the phase transition and the critical behaviour for two different concentratio.
Cu^{2+} ions, i.e. 0.043 wt% and 0.98 wt%, we have recorded the EPR signal intensity
the sample is cooled or warmed at a rate of 0.5 °C per 100 min, every 0.1 °C (δT) interva.
around the phase transition. At a given temperature the sample is maintained for a long
time to ensure that no further change in EPR signal intensity takes place. $\delta T/T_{c1}$ is about
5×10^{-4} and therefore the critical phenomena can be studied from such measurements.
The plot of normalised intensity I with temperature thus recorded is shown in figures
5(a) and 6(a). Figures 5(b) and 6(b) show the plots of log (I/I_m) versus log ε, where $\varepsilon =
|1 - T/T_{c1}|$. In figure 5(b), I_m corresponds to the transition at the point A. Three points
on this plot which are obtained for the points A, B, C and D in figures 5(a) (where the
temperature differences between the point A and the points B, C and D are taken to be
0.1 °C, 0.2 °C and 0.3 °C, respectively) lie in a straight line with a slope β of 0.5 $\pm$ 0.05,
for the Cu^{2+} concentration of 0.043%. Thus, for this low concentration, mean-field-type
behaviour is observed. However, for the higher Cu^{2+} concentration (0.98 wt%), the plot
(figure 6(b), line 1) for the points A, B, C, D and E is shown by full circles and a full line
to guide the eye (here, the temperature differences between the point A and the points
B, C, D and E are taken to be 0.1 °C, 0.2 °C 0.3 °C and 0.4 °C, respectively). I_m
corresponds to the minimum intensity observed at the transition corresponding to the
point A. The corresponding slope β of the line is 0.17 $\pm$ 0.05. However, if we take the
exact temperature differences between the point A and the points C, D and E as shown
in the graph, we obtain the plot (figure 6(b), 2) shown by the three circles with dots in.
The corresponding slope β of the straight line passing through these points is 0.12 $\pm$ 0.03.
The EPR signal intensity I may be related to the order parameter of the phase transition,
which is related to the orientation and tetragonal distortion of the TiF$_6^{2-}$ group at the
transition (Bose et al 1983, Afanasyev et al 1979) and β may be taken as the critical
exponent in the relation $I/I_m = \varepsilon^{\pm\beta}$. As determined in this experiment, the value of β
lies between 0.17 and 0.12 for the 0.98 wt% Cu^{2+} concentration; however, the preferred
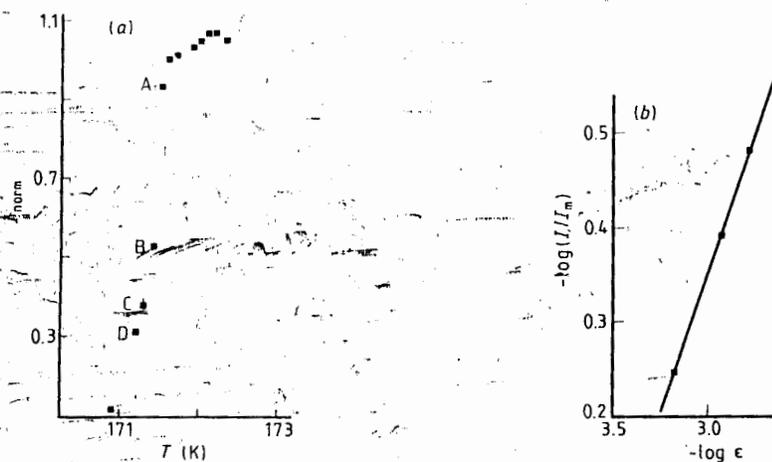

Figure 5. (a) The plot of the normalised isotropic EPR signal intensity (normalised with
respect to the maximum EPR intensity immediately before the transition starts) with tem-
perature change in the immediate neighbourhood of T_{c1} while cooling from the high-
temperature phase (the Cu^{2+} concentration in ZTFH is 0.043 wt%); (b) the plot of log ε versus
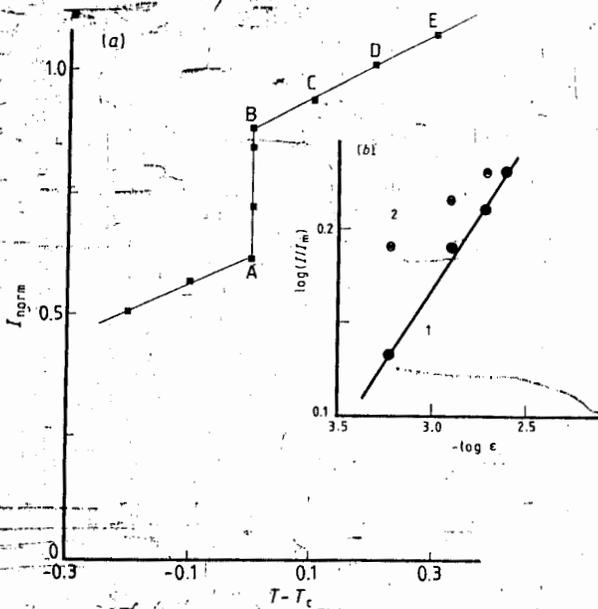log(I/I_m) (see text).

Figure 6. (*a*) The EPR signal intensity in the immediate neighbourhood of T_{c1} for a Cu^{2+} concentration of 0.98 wt% in ZTFH ($T_{c1} = 108.7\,°C$); (*b*) the plot of log ε versus $\log(I/I_m)$ (see text).

value is 0.12. Thus, we see that, with a high JT impurity concentration, there is a deviation from mean-field behaviour. This feature is under further study using different Cu^{2+} concentrations and Ni^{2+} concentrations in ZTFH as well as in ZTFD.

5. The Jahn–Teller potential splitting

The sharp drop in the isotropic EPR signal intensity I may be related to the JT potential splitting E_0; from our earlier work on JT systems of ZTFH : Cu and $MgSiF_6 \cdot 6H_2O$: Cu (Rubins *et al* 1984), it is established that the three JT potential wells (corresponding to JT distortions along the x, y, z axes of the $[Cu^{2+} \cdot 6H_2O]$ complex are equivalent in the trigonal phase (figure 7(*a*)).
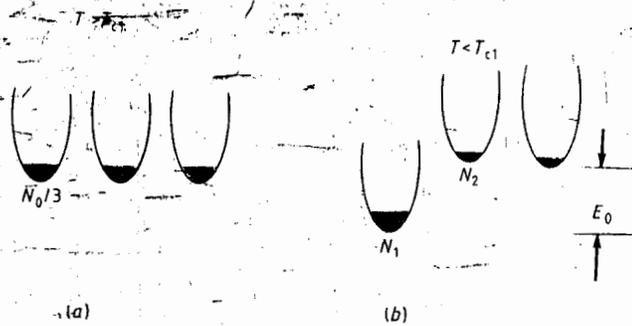

Figure 7. Schematic picture showing that the JT potential wells are non-equivalent by an energy E_0 below T_{c1}.

However, below T_{c1}, i.e. in the monoclinic phase, the wells are non-equivalent by an energy E_0 (figure 7(b)). The energy E_0 has been determined previously (De 1984) for very low Cu^{2+} concentrations (0.043 wt%) from temperature variations in the spin Hamiltonian parameters $g_{\parallel}$, $g_{\perp}$, $A_{\parallel}$ and $A_{\perp}$ down to 4.2 K. It should be noted that E_0 is not the same as the JT stabilisation energy E_{JT}.

In the following, we show that it is also possible to determine E_0 from the observed abrupt drop in EPR intensity at T_{c1}. When the sample is cooled from the high-temperature phase, we assume that, at T_{c1}, one of the three JT potential wells becomes lower than the other two by an energy E_0 (figure 7(b)), i.e. the initial splitting occurs at T_{c1} although, below T_{c1}, E_0 may increase with decrease in temperature. The energy separation between the other two wells is much smaller than E_0 and we neglect it in the following calculations. It should be noted that these three wells are actually warped and the minima are separated by 120°, 240° in the plane of Q_θ, Q_η; Q_θ, Q_η are the normal coordinates of the complex transforming as d_{z^2} and $d_{x^2-y^2}$ of $3d^9$ wavefunctions. The isotropic EPR signal in a JT system in general is due to rapid tunnelling or phonon-induced reorientation among the three wells; it may also arise because of the population of the vibronic levels $^2A_2$ or $^2A_1$ (Ham 1972). In ZTFH : Cu^{2+}, the populated level $^2A_2$ level seems to give rise to the isotropic signal (De 1986).

When the measurement is made along one of the three [100] directions, the EPR signal intensity is proportional to the ground-state population of the $^2A_2$ state in one of the wells in figure 7(a), i.e. for $T = T_{c1} + \delta$

$$\lim_{\delta \to 0} (I_{T_{c1}+\delta}) = \tfrac{1}{3}CN_0. \tag{1}$$

C is the proportionality constant. N_0 is the total population of the $^2A_2$ state in the three wells at T_{c1}. This is based on the fact that the tunnelling frequency is smaller than the microwave frequency. Otherwise, the factor $\tfrac{1}{3}$ in equation (1) should be omitted. It may be mentioned that the spin–lattice relaxation rate $1/T_1$ calculated from equation (6) of the paper by De (1986) is found to be about $6 \times 10^6\,s^{-1}$. $1/T_1$, which includes contribution from the phonon-induced reorientation and tunnelling among the three JT wells, is much smaller in the present system than in JT systems (see §1) exhibiting no structural transition (De 1986). Using the approximate R value found by Dang et al (1974) of $(1/T_1)/(1/\tau) = 6.4 \times 10^{-3}$ for the (100) orientation in $ZnSiF_6.6H_2O : Cu^{2+}$, we can approximately estimate the value of the tunnelling rate $1/\tau$ at T_{c1} in ZNTFH : Cu^{2+} to be $0.94 \times 10^9\,s^{-1}$, much less than the microwave frequency of 35 GHz employed in this work. Below the transition point T_{c1}, the population distributions in the three wells as described in figure 7(b) are as follows:

$$N_2 = N_1 \exp(-E_0/kT). \tag{2}$$

$$N_1 + 2N_2 = N_0 \tag{3}$$

Thus,

$$N_2 = N_0 \exp(-E_0/kT)/[1 + 2\exp(-E_0/kT)]. \tag{4}$$

Tunnelling may still be present among these wells. However, now N_1 corresponds to the anisotropic EPR signal because, with a lowering of the temperature below T_{c1}, N_1 increases at the expense of N_2. This is reflected in the observed increase in anisotropic signal intensities at the expense of the isotropic signal intensity I. So, we can say that the isotropic signal intensity I immediately below the transition still corresponds to the

lation N_2 of the $^2A_2$ state in one of the two upper wells and we have

$$\lim_{\sigma \to 0} (I_{T_{c1-\sigma}}) = CN_2. \tag{5}$$

Thus, from equations (1), (4) and (5), we obtain

$$r = \lim_{\sigma \to 0} (I_{T_{c1-\sigma}}/I_{T_{c1+\sigma}}) = 3x/(1 + 2x) \tag{6}$$

where $x = \exp(-E_0/kT_{c1})$. Equation (6) tells us that, if $E_0 = 0$ at T_{c1}, we expect continuous transition. If $E_0 = \infty$ at the transition, we expect ideal abrupt transition. For intermediate E_0, we expect transitions whose nature lies between 'ideal continuous' and 'ideal abrupt'.

Let us see how this model allows us to evaluate E_0 from the observed variations in the isotropic signal intensity I in figures 5 and 6 for Cu^{2+} concentrations of 0.043 and 0.98 wt% in ZTFH. We determine from these figures that the corresponding values of r are 0.56 ± 0.04 and 0.70 ± 0.05, with the corresponding transition temperatures T_{c1} being 171.5 K and 164.5 K, respectively. We then determine from equation (6) that the corresponding values of E_0 are 140 ± 14 cm^{-1} and 94 ± 11 cm^{-1}, respectively. This means that for higher concentrations the splitting E_0 will decrease. From equations (4) and (5), below T_{c1} but for temperatures close to T_{c1}, $z = (\mathrm{d}I/\mathrm{d}T)/I \propto E_0/kT_{c1}^2(1 + 2x)$ where we neglect terms such as $\exp(-g\mu_B H/kT)$, which is important only at low temperatures (less than 4.2 K). z decreases with decrease in E_0, which means that, as E_0 decreases with increase in Cu^{2+} concentration, the transition may become gradual with respect to temperature. The observed gradual transition (gradual in the sense that the isotropic signal due to the trigonal phase of ZTFH continues to exist over a finite temperature interval, which increases with increasing Cu^{2+} concentration) for high Cu^{2+} concentrations (figure 4) is thus consistent with the above model.

6. Effect of deuteration

We have repeated the above experiment and analysis for a ZTFD crystal containing a low Cu^{2+} concentration. The transition is found to be gradual with respect to temperature as seen from figure 8, unlike the hydrated crystal containing a low Cu^{2+} concentration. T_{c1} may be noted to be $-105.5\,°C$ where there is clearly a significant change in the isotropic signal intensity from that at $-105\,°C$. This is accompanied by the appearance of signals (anisotropic) on the high-field side as well as on the low-field side. The value of r in equation (6) may be taken to be the ratio in figure 8 of the EPR intensities at -105.5 and $-105\,°C$. r is determined to be 0.78 ± 0.017. With $T_{c1} = 167$ K, we then obtain from equation (6) that $E_0 = 77 ± 9$ cm^{-1}. This value of E_0 is consistent with the gradual transition observed in this crystal. An experimental study on the critical behaviour in the deuterated crystal containing different Cu^{2+} and Ni^{2+} concentrations is in progress. If the same correlation exists in the deuterated crystal, then we should expect decreasing values of the critical exponent β and the splitting of E_0 with increasing Cu^{2+} concentration. Moreover, the value of the critical exponent in the deuterated crystal for a given Cu^{2+} concentration should be smaller than that in the hydrated crystal. In general, a smaller critical exponent means that the dimensionality of the system at the phase transition is low, and gradual or continuous transition can be expected.
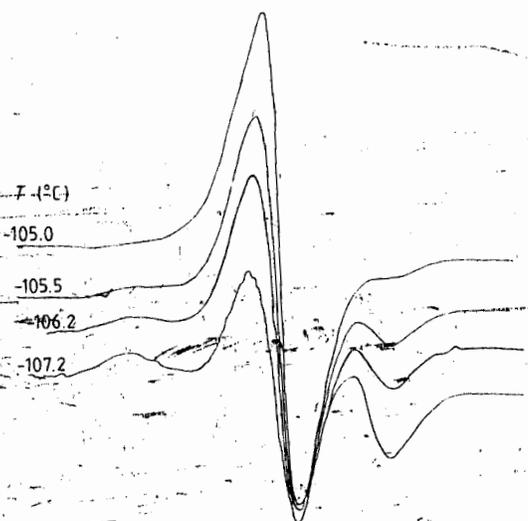
Figure 8. EPR spectrum of Cu^{2+} in ZTFD showing that deuteration changes the nature of the phase transition from abrupt to gradual (compare with figure 1 and see text). The E_0 value is much lower than that of the hydrated crystal.

7. Conclusion

The origin of E_0 may be said to lie in the monoclinic distortion of the host lattice, i.e. ZTFH at T_{c1}. So E_0 is a measure of the distortion. For no structural transition, E_0 should be zero or very small. The fact that E_0 as well as β are smaller for higher JT impurity concentrations might mean that the higher JT impurity concentration is offering resistance to the lattice from undergoing a structural transition. Physically, this means that T_{c1}, the temperature at which the soft mode frequency of the system becomes zero, is strongly dependent on the presence of a JT impurity, indicating a coupling of the soft mode to the JT modes. Since the sharp transition at T_{c1} is associated with the tetragonal distortion of the TiF_6^{2-} octahedra (Chowdhury *et al* 1981, 1985) and the weak continuous transition at $-56\,°C$ is associated with the tilt of the $[M^{2+}, H_2O]$ octahedra, and since the high Cu^{2+} concentration tends to make the transition at T_{c1} continuous or gradual with temperature, it is possible that the JT impurity concentration is influencing the coupling of the modes associated with these two units which constitute the crystal ZTFH in a CsCl packing. It should be noted that in pure ZTFD the transition at T_{c2} ($-43\,°C$) is of a more continuous nature than that of pure ZTFH. At T_{c2} the tilt of the water octahedra constitutes the soft mode. When this is combined with our observation of gradual transition at T_{c1} in ZTFD even for low Cu^{2+} concentrations, we also see that coupling of the above two modes via a JT impurity is possible. However, the fundamental questions of how the JT effect influences the said coupling and the dimensionality of phase transition in this crystal remain to be theoretically investigated. It is also not understood whether the decrease in transition temperature T_{c1} in powdered material (containing a low Cu^{2+} concentration (De 1986)) has the same underlying cause as the decrease in T_{c1} in crystals containing a high Cu^{2+} concentration. It may appear that in powdered material the short-range correlation of the soft mode rather than the long-range correlation would be predominant, while in single crystals with high Cu^{2+} concentrations the soft mode would

expected to have long-range correlation, because of the possible interaction between the soft mode and the JT active modes (Hock and Thomas 1977). Determinations of the critical exponent and the JT potential splitting E_0 for many different Cu^{2+} and Ni^{2+} concentrations in hydrated and deuterated crystals are necessary before we can throw sufficient light on the separate role of JT and non-JT impurities in the dynamics of structural transition and the above apparent contradiction in this material. Raman scattering and IR studies will be of additional help to elucidate the interaction of the different modes associated with the $[M, H_2O]^{2-}$ and TiF_6^{2-} at the transition (Chowdhury *et al* 1983). Further useful studies will concern the application of uniaxial stress and study the changes in transition temperatures, the critical exponent and the JT splitting E_0.

Acknowledgments

References

Afanasyev M L, Lybzikov A F, Menshikov V V and Zeer E P 1979 *Chem. Phys. Lett.* **60** 279
Bose M, Roy K and Goshray A 1983 *J. Phys. C: Solid State Phys.* **16** 645–50
Chowdhury P, Bal B, Saha S and Ghosh B 1981 *Proc. NP and SSP Symposium India* **24C** 323
Chowdhury P, Ghosh B, Lamba C P and Bist H D 1983 *J. Phys. C: Solid State Phys.* **16** 1609
Chowdhury P, Ghosh B, Patel M B and Bist H D 1985 *J. Raman Spectrosc.* **16** 149
Dang L S, Buisson R and Williams F I B 1974 *J. Physique* **35** 49
Das A N, Chowdhury P and Ghosh B 1985 *J. Phys. C: Solid State Phys.* **18** 5975
De D K 1986 *Phys. Rev.* B **34** 4651
De D K, Rubins R S, Black T D 1984 *Phys. Rev.* B **29** 71
Ham F S 1972 *Electron Paramagnetic Resonance* ed. S Geschwind (New York: Plenum) pp 1–119
Hock K H and Thomas H 1977 *Electron–Phonon Interactions and Phase Transitions* ed. T Riste (New York: Plenum) p 271
Kodera E, Torii A, Osaki K and Watanabe T 1972 *J. Phys. Soc. Japan* **32** 863
Rubins R S 1974 *Chem. Phys. Lett.* **28** 273
Rubins R S and Black T D 1981 *Chem. Phys. Lett.* **81** 450
Rubins R S, Tello L N, De D K and Black T D 1984 *J. Chem. Phys.* **81** 4230
Syoyama S and Osaki K 1972 *Acta Crystallogr.* B **28** 2626